SUPPLEMENTARY INFORMATION

A Comprehensive Experimental and Computational Spectroscopic Study of Hexacyanoferrate Complexes in Water: from the Infrared to X-ray Wavelengths

Matthew Ross,[⊥†] *Amity Andersen,*[□] *Zachary W. Fox,*[⊥] *Yu Zhang,*[■†] *Kiryong Hong,*[▲†] *Jae-Hyuk Lee,*[▲†] *Amy Cordones,*[▲†] *Anne Marie March,*[◊] *Gilles Doumy,*[◊] *Stephen H. Southworth,*[◊] *Matthew A. Marcus,*[○] *Robert W. Schoenlein,*[▲†] *Shaul Mukamel,*[■] *Niranjan Govind*[□*] *and Munira Khalil*[⊥*]

[⊥] Department of Chemistry, University of Washington, Seattle, WA 98115, USA

[□] Environmental Molecular Sciences Laboratory, Pacific Northwest National Laboratory, P.O. Box 999, Richland, WA 99352, USA

[■] Department of Chemistry, University of California, Irvine, CA 92697, USA

[▲]Ultrafast X-ray Science Laboratory, Chemical Sciences Division, Lawrence Berkeley National Laboratory, Berkeley, CA 94720, USA

[◊] Chemical Sciences and Engineering Division, Argonne National Laboratory, Argonne, IL 60439, USA

[○]Advanced Light Source, Lawrence Berkeley National Laboratory, Berkeley, CA 94720, USA

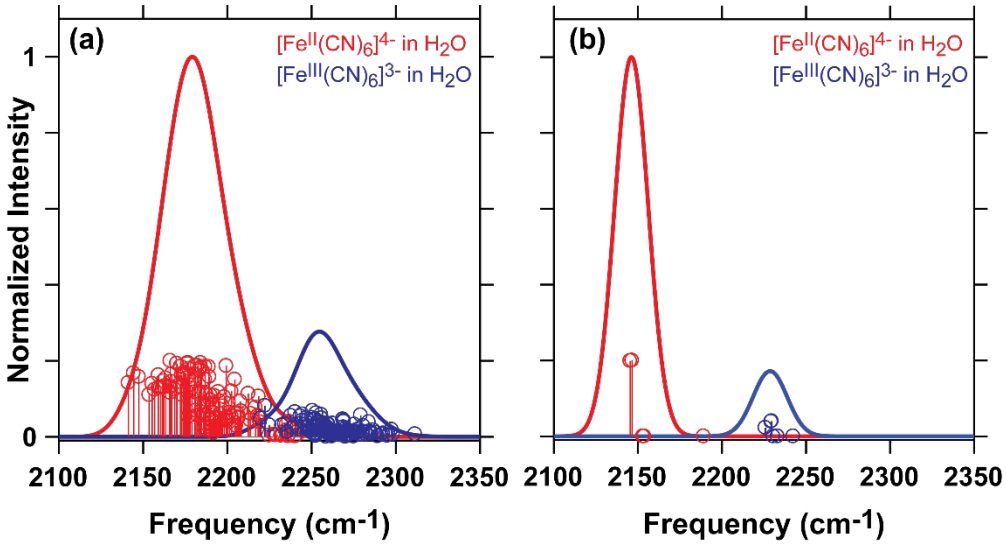

Figure S1. IR spectra from simulation using different models of solvation for the Fe(II) and Fe(III) complexes dissolved in water. (a) Vibrational spectra calculated using a harmonic analysis of 20 snapshots from the QM/MM simulations. See main text for details. (b) The COSMO calculations were performed on an optimized cluster with perfect octahedral symmetry.

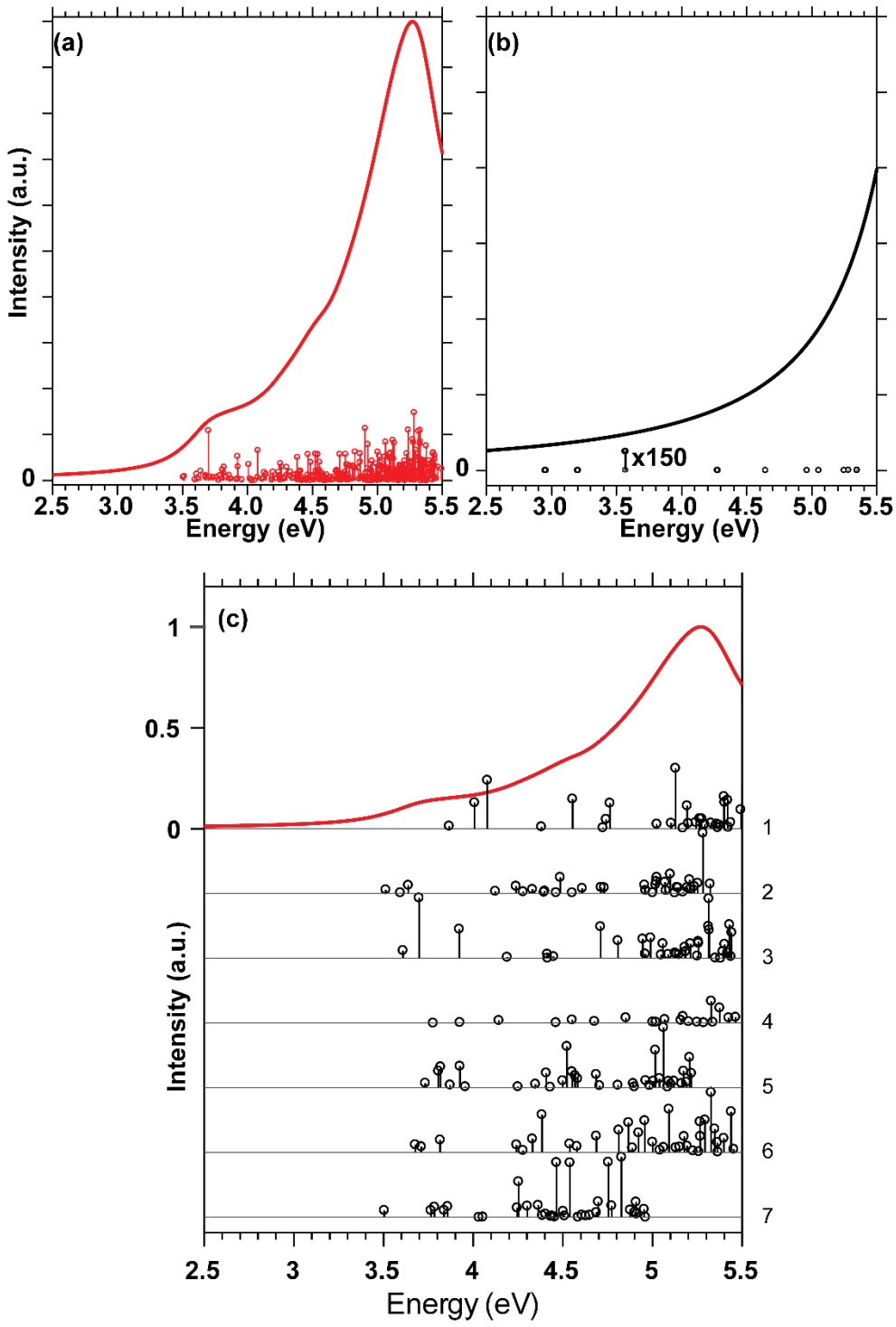

Figure S2 UV/Vis spectra from simulation using different models of solvation for the Fe(II) complex dissolved in water. (a) The calculations are performed using explicit solute-solvent configurations. See the main text for details. (b) The COSMO calculations were performed on an optimized cluster with perfect octahedral symmetry. (c) The stick spectra for seven representative clusters including explicit solute-solvent interactions are shown labeled 1-7 under the averaged spectrum.

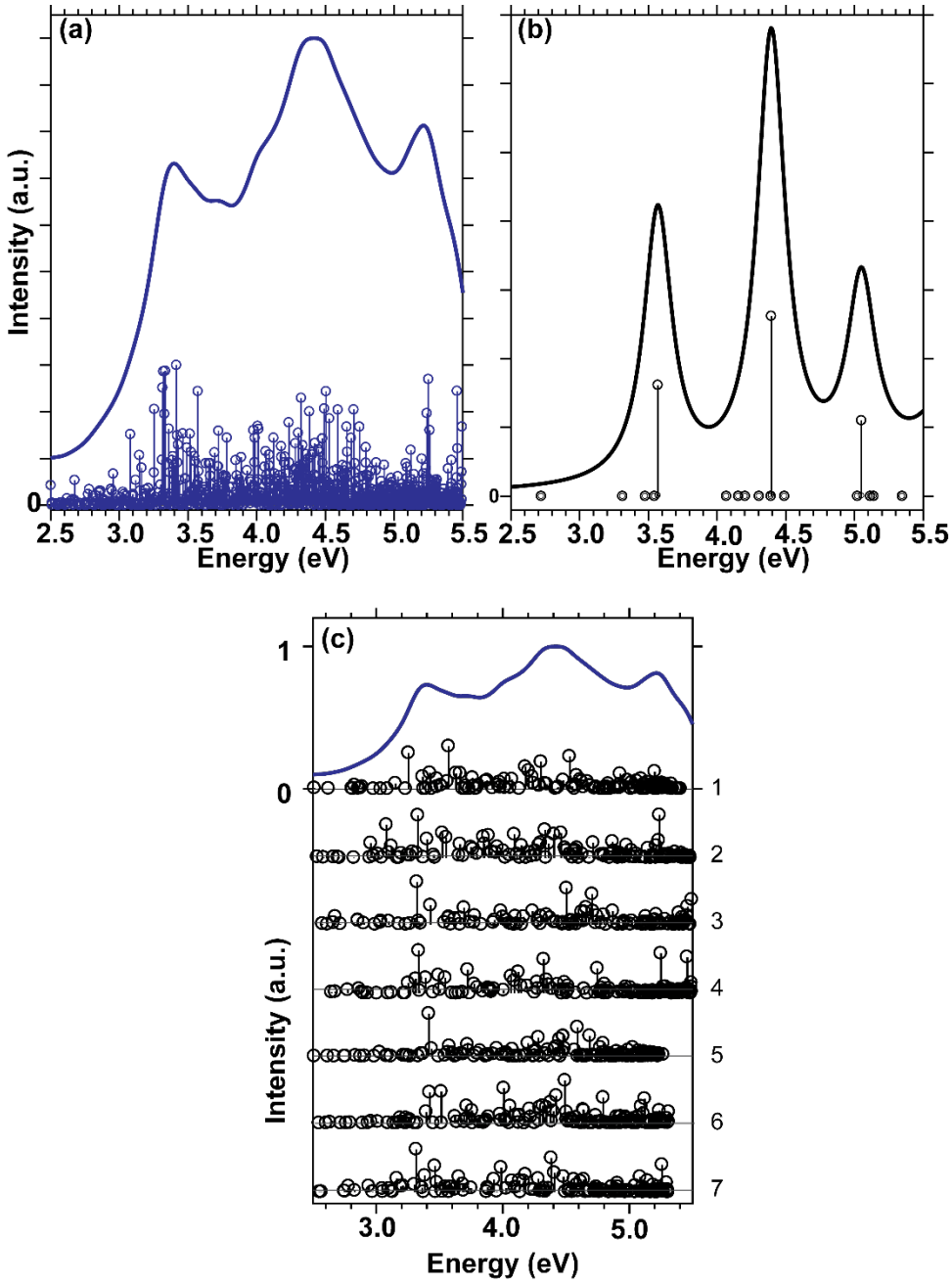

Figure S3. UV/Vis spectra from simulation using different models of solvation for the Fe(III) complex dissolved in water. (a) The calculations are performed using explicit solute-solvent configurations. See the main text for details. (b) The COSMO calculations were performed on an optimized cluster with perfect octahedral symmetry. (c) The stick spectra for seven representative clusters including explicit solute-solvent interactions are shown labeled 1-7 under the averaged spectrum.

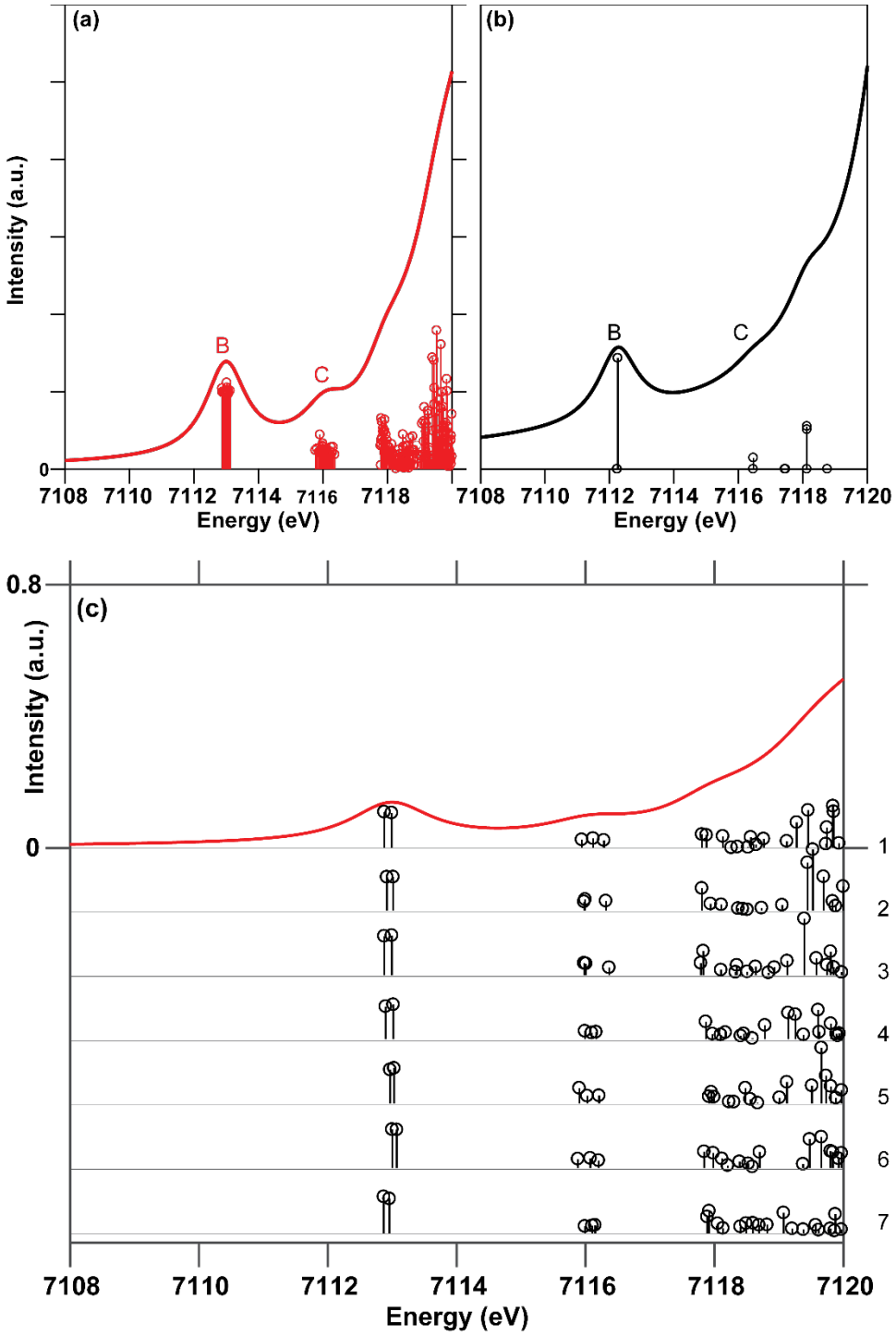

Figure S4. Fe K-edge XANES spectra from simulation using different models of solvation for the Fe(II) complex dissolved in water. Both spectra have been shifted by +143.0 eV. (a) The calculations are performed using explicit solute-solvent configurations. See the main text for details. (b) The COSMO calculations were performed on an optimized cluster with perfect octahedral symmetry. (c) The stick spectra for seven representative clusters including explicit solute-solvent interactions are shown labeled 1-7 under the averaged spectrum.

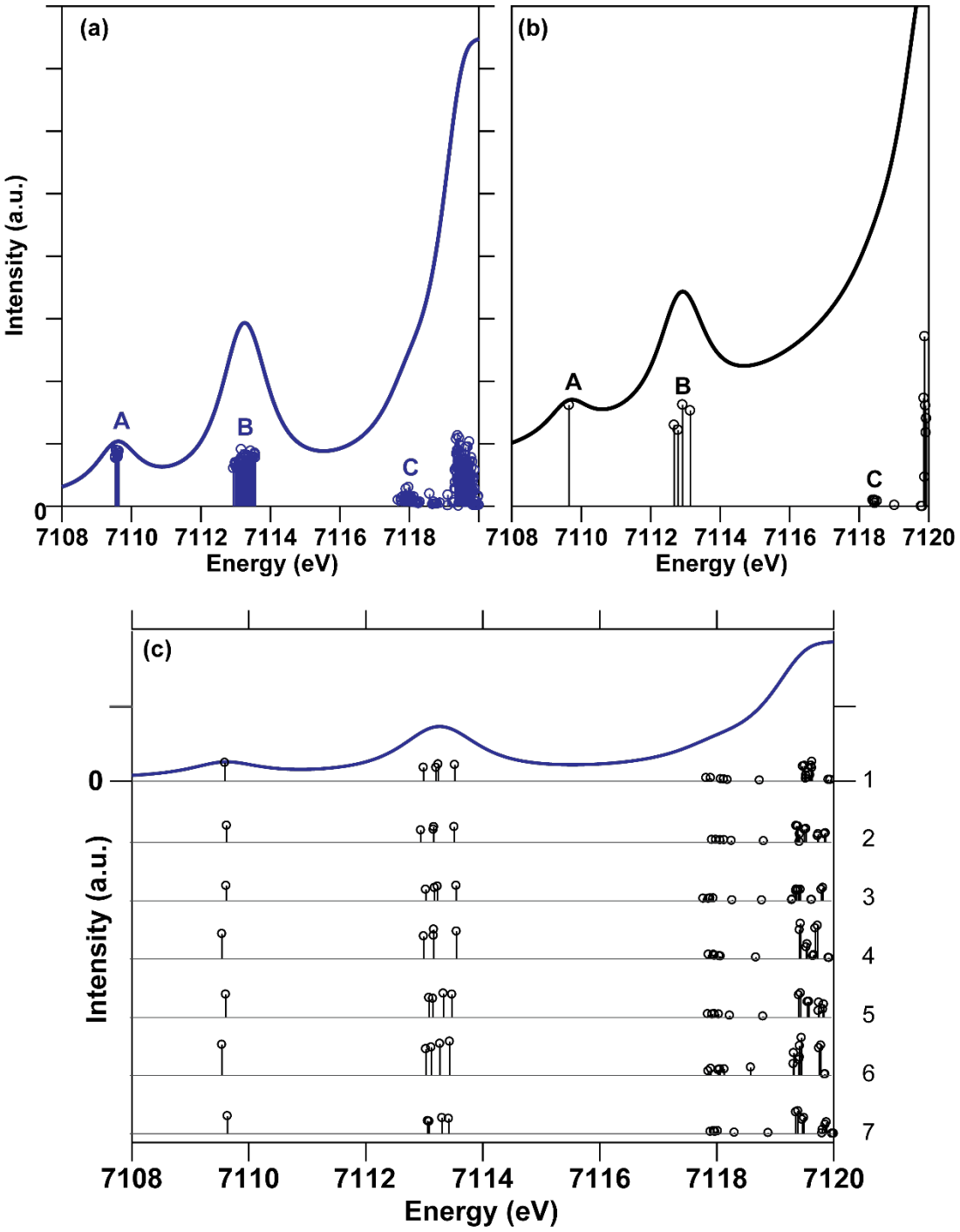

Figure S5. Fe K-edge XANES spectra from simulation using different models of solvation for the Fe(III) complex dissolved in water. Both spectra have been shifted by +143.0 eV. (a) The calculations are performed using explicit solute-solvent configurations. See the main text for details. (b) The COSMO calculations were performed on an optimized cluster with perfect octahedral symmetry. (c) The stick spectra for seven representative clusters including explicit solute-solvent interactions are shown labeled 1-7 under the averaged spectrum.

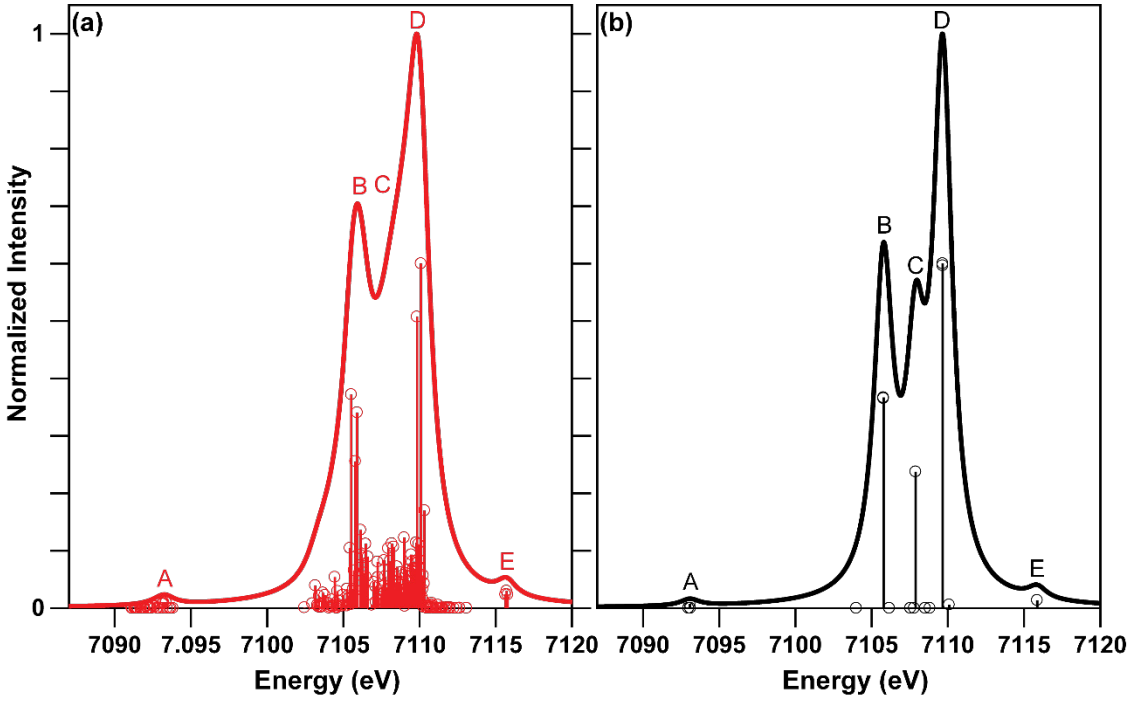

Figure S6. Fe K-edge valence to core X-ray emission spectra from simulation using different models of solvation for the Fe(II) complex dissolved in water. Both spectra have been shifted by -10.1 eV. (a) The calculations are performed using an explicit solute-solvent configuration. See the main text for details. (b) The COSMO calculations were performed on an optimized cluster with perfect octahedral symmetry.

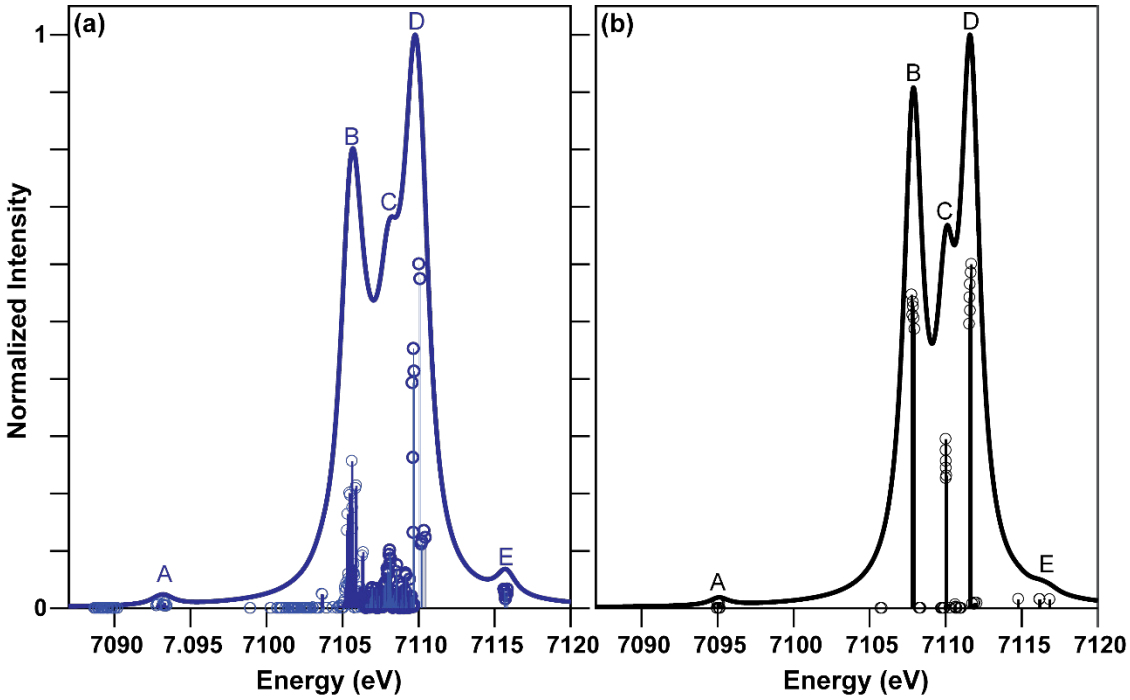

Figure S7. Fe K-edge valence to core X-ray emission spectra from simulation using different models of solvation for the Fe(III) complex dissolved in water. Both spectra have been shifted by -10.1 eV. (a) The calculations are performed using an explicit solute-solvent configuration. See the main text for details. (b) The COSMO calculations were performed on an optimized cluster with perfect octahedral symmetry.

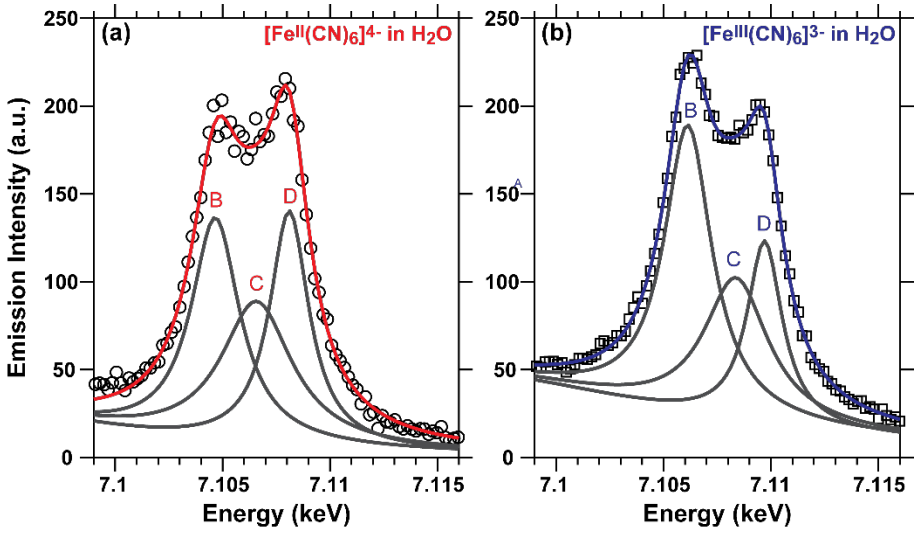

Figure S8. Expanded view of the experimental VtC-XES spectra of hexacyanoferrate complexes dissolved in water. The black circles and squares are the experimental data. The solid lines are fits of the data to a sum of pseudo-Voigt line shapes. The labels B-D refer to peaks discussed in the main text.

Fe(II): MOs contributing to Feature C

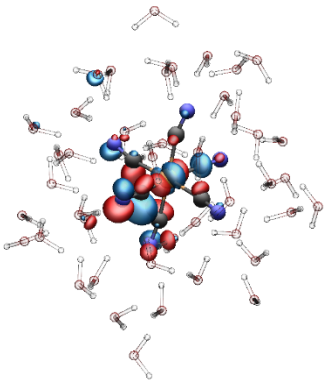

MO 283

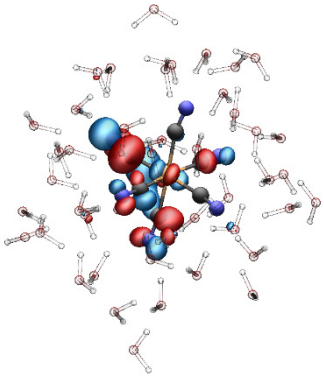

MO 285

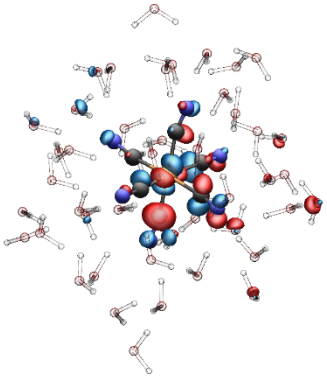

MO 289

Fe(III): MOs contributing to Feature C

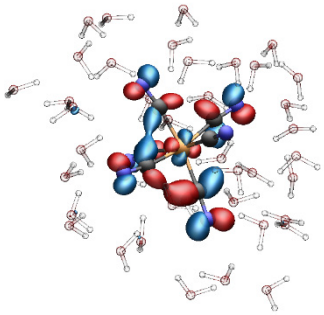

MO 265(α)

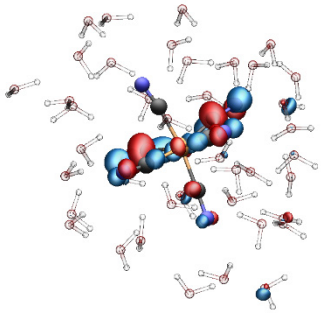

MO 263(α)

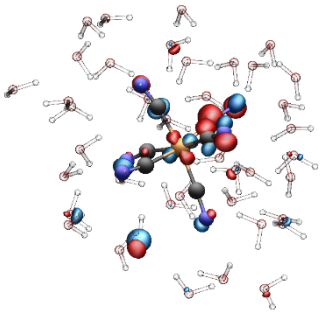

MO 266(β)

Figure S9. Molecular orbitals contributing to the intensity for transitions comprising Feature C in the Fe(II) and Fe(III) complexes. Red corresponds to positive electron density and blue corresponds to negative electron density.

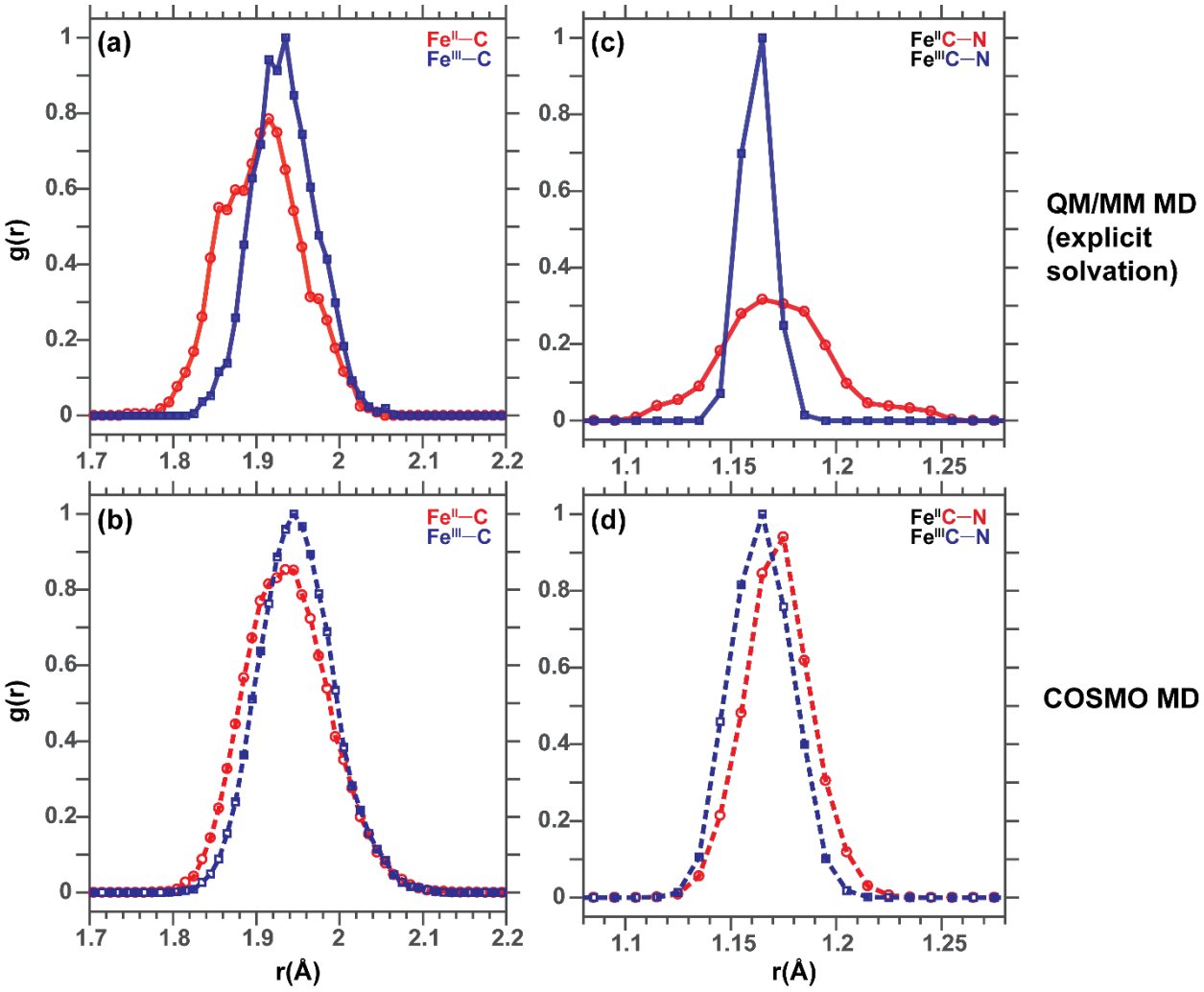

Figure S10. Pair distribution functions, g(r) for the (a-b) Fe-C bond lengths and (c-d) C≡N bond lengths. Red: $[Fe^{II}(CN)_6]^{4-}$ complex; Blue: $[Fe^{III}(CN)_6]^{3-}$ complex. The pair distribution analysis for (a) and (c) are performed using explicit solvation in QM/MM MD simulations as described in the main text. The pair distribution analysis for (b) and (d) is performed using an implicit solvation model in COSMO MD simulations. COSMO MD simulations with the PBE0 exchange-correlation functional were performed with the Gaussian basis AIMD module for finite systems implemented in NWChem (Fischer, 2016). Simulations on both complexes were run for 20 ps after equilibration (~1 ps) at 298.15 K using the stochastic velocity rescaling (SVR) thermostat (Bussi, 2007). As with the QM/MM simulations, C and N atoms were described with the 6-311G** basis set and the Fe atom was described with the Stuttgart basis set/relativistic small-core effective core potential, respectively.

Table S1. Best-fit parameters extracted from the fit of the EXAFS data for the Fe(II) and Fe(III) complexes dissolved in water. Only the parameters from the single scattering paths are reported because the parameters for the multiple scattering paths were correlated with those from the single scattering path.

Compound	**R_{Fe-C}, Å (Single Scattering Path)**	**R_{Fe-N}, Å (Single Scattering Path)**	**σ^2, Å^2 (Fe-C)**	**σ^2, Å^2 (Fe-N)**	**S_0^2**
$[Fe(CN)_6]^{4-}$	1.92±0.01	3.11±0.01	0.0016±0.0004	0.0072±0.0004	0.71±0.03
$[Fe(CN)_6]^{3-}$	1.94±0.01	3.13±0.01	0.0026±0.0006	0.0090±0.0006	0.80±0.01

References:

Fischer, S. A.; Ueltschi, T. W.; El-Khoury P. Z.; Mifflin A. L.; Hess, W. P.; Wang H.F; Cramer,C. J.; Govind N. Infrared and Raman Spectroscopy from Ab Initio Molecular Dynamics and Static Normal Mode Analysis: The CH Region of DMSO as a Case Study. J. Phys. Chem. B, 2016, 120 (8), 1429–1436.

Bussi, G.; Donadio, D.; Parrinello, M., Canonical Sampling Through Velocity Rescaling. J. Chem. Phys. 2007, 126, 014101.